

Research Article

Reduction of Background Fluorescence from Impurities in Protein Samples for Raman Spectroscopy

Marco Pinto Corujo ¹, Pavel Michal ², Rod Wesson,¹ Don Praveen Amarasinghe,¹ Alison Rodger ³, and Nikola P. Chmel ¹

¹MAS, Centre for Doctoral Training, University of Warwick, CV4 7ALUK, Coventry, UK

²Department of Optics, Palacký University Olomouc, 17. listopadu 12, Olomouc 77146, Czech Republic

³School of Natural Sciences, Macquarie University, Sydney, NSW 2109, Australia

Correspondence should be addressed to Marco Pinto Corujo; marco.pinto@agilent.com

Received 7 April 2022; Revised 10 October 2022; Accepted 13 October 2022; Published 24 November 2022

Academic Editor: Mohd Sajid Ali

Copyright © 2022 Marco Pinto Corujo et al. This is an open access article distributed under the Creative Commons Attribution License, which permits unrestricted use, distribution, and reproduction in any medium, provided the original work is properly cited.

Background fluorescence remains the biggest challenge in Raman spectroscopy because of the consequent curvature of the baseline and the degradation of the signal-to-noise ratio of the Raman signal. While the concentrations of the fluorophore impurities are usually too low to be detected by other analytical methods, they are often sufficient to prevent Raman data collection. Among the different existing methods to remove the fluorescence signal, photobleaching remains the most popular due to its simplicity. However, using the spectrometer laser to photobleach is far from optimal. Most commercially available instruments have little or no choice of wavelength, and their output powers are in many cases not suitable for highly fluorescent samples such as those from biological systems (e.g., proteins). In this article, we assess practical aspects of photobleaching such as the apparent reversibility of the process and the effect of convection currents due to what we speculate to be temperature gradients across the bulk of the solution. We also introduce an affordable custom made external photobleaching unit with a choice of excitation wavelength and demonstrate its viability with a highly fluorescent bovine serum albumin protein solution, which had proved most challenging for Raman spectroscopy as it contained ~10% w/w impurities.

1. Introduction

Many studies in the field of molecular analytical science are carried out with biological samples, which have been treated to extract the desired components (e.g., DNA, RNA, lipids, and proteins) [1, 2]. Although these molecules are put through different purification procedures, e.g., ion exchange chromatography, affinity chromatography, gel filtration, and gel electrophoreses, to separate them from one another and other cellular components, trace concentrations of impurities often remain in the sample in addition to the molecules of interest, proteins in our case [2, 3]. Because Raman spectrometers measure all the Stokes shifted frequencies that reach the detector, whether it is from Raman or other phenomena, and because fluorescence has a yield several orders of magnitude larger than that of inelastic scattering,

even a very low concentration of fluorescent impurities in the sample can cause significant background fluorescence [1, 4]. Among the main effects caused by fluorescence in a Raman measurement are the degradation of the signal-to-noise ratio, the rise of a broad Gaussian shaped baseline, and the saturation of the detector that in extreme cases can completely mask the signals of interest [5–7].

Fluorescence can be quenched by adding components with different molecular interactions such as energy transfer, ground-state complex formation, and collisional quenching [8, 9]. They are based on different physical-chemical interactions between a quenching agent and the fluorophore that results in a lower fluorescence quantum yield and therefore fluorescence intensity [8]. Quenching effects can be reversed by removing the quenching agent. Moreover, simple filtration to remove solid particles suspended in a solution removes

their contribution to the background due to both fluorescence and Mie scattering [10, 11], and thus it is advisable to filter samples with syringe filter disks (ideally membranes should have pore size $<0.45\ \mu\text{m}$) prior to Raman measurements [12]. An alternative approach to suppress fluorescence is by means of excited state reactions and molecular rearrangements of the fluorescent impurity when exposed to UV-Vis light that results in degradation of fluorophores in a phenom referred to as photobleaching [13]. Photobleaching is the most extensively used fluorescence suppressing technique in Raman spectroscopy because of its simplicity. Although the molecular pathways by means of which photobleaching occurs are not well understood, some authors have suggested that the fluorophore might undergo an intersystem crossing and that, because of the longer life time of the triplet state compared to that of the singlet, a second photon could be absorbed causing it to transit to a higher energy state from which it could react with other molecules in the surroundings [14, 15]. The molecules that cause fluorescence interference in a Raman spectrum are typically impurities that absorb at the excitation wavelength, reason why they can be photobleached by simply exposing them to the laser. Shorter wavelengths may be more effective. However, proteins contain aromatic side chains with absorption bands in the range 250–290 nm. The wavelength of choice for photobleaching should be far from exciting any chromophores in the analyte if its integrity wants to be preserved. Although some impurities will also have a resonance Raman signal, they are always present at very low levels (not apparent in a standard fluorimeter). The low concentrations together with the fact that even resonance Raman scattering is several orders of magnitude smaller than fluorescence mean that the impurities should not be observable in the Raman spectrum.

The decay of background fluorescence for any given fluorophore in a light beam with time has been reported to fit an exponential decay and the rate is believed to depend on the laser power and the excitation wavelength used [13, 16]. Photobleaching proceeds by destroying the fluorophores and as such the process is irreversible. However, as those changes are localised to the irradiated parts of the sample, the migration of fluorophores from non-irradiated parts of the samples leads to gradual recovery of background fluorescence over time, when the laser exposure ceases. This leads to apparent “reversibility” of the process. We also noted another phenom that contributes to apparent “reversibility” in the form of irregular rebounds of the background fluorescence after extended periods of photobleaching. We speculate this is due to convective currents resulting from temperature gradients.

As we have found that biological samples, in pharmacologically relevant concentration ranges, often display amounts of background fluorescence that makes spectra acquisition impossible, there is no option but to suppress the fluorescence which requires significant amounts of photobleaching. This generally cannot be dealt with by means of conventional benchtop instruments due to their low output laser powers, the lack of excitation wavelength choice, and the removal of the instrument from data collection while it is photobleaching.

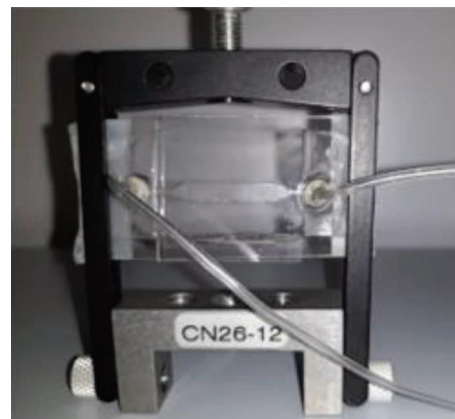


FIGURE 1: Polydimethylsiloxane channel with an inlet and outlet.

In this paper, we review some of the characteristics of the photobleaching process and introduce and assess an external photobleaching unit designed to help minimise instrument time when measuring extremely fluorescent samples.

2. Materials and Methods

2.1. Samples and Reagents. A $\sim 40\ \text{mg}\cdot\text{ml}^{-1}$ stock solution in water (18.2 M Ω , Millipore) of bovine serum albumin (BSA, Sigma-Aldrich, Poole, UK) was prepared and diluted to accommodate to the optical density requirements of the different instruments used (see Experimental Procedures).

2.2. Instrumentation. A FP-6500 fluorimeter (Jasco, UK), a DXR2 Smart Raman spectrometer (Thermo Fisher, UK) equipped with a 633 nm He laser ($\sim 8\ \text{mW}$ power at sample position), and a ChiralRAMAN-2X™ ROA spectrometer (BioTools, USA) equipped with a 532 nm Nd-YAG laser ($\sim 2000\ \text{mW}$ at control unit, $\sim 55\%$ at sample position) were used.

A simple PDMS (Dow Corning Sylgard 184 silicone elastomer) microfluidic channel (Figure 1) was prepared using standard lithographic methods [17] to a depth of approximately 1.5 mm, with channel dimensions as specified in the “Supplementary Materials” section (Figure S1). Access holes for the fluid to enter the channel were drilled into the PDMS using a biopsy puncher. The PDMS above the main chamber of the fluid channel was cut out with a scalpel, and two quartz microscope slides were bonded to the microfluidic device to create a rigid fluid flow cell. The bonding was performed by exposing the PDMS microfluidic device and the quartz slides to oxygen plasma, placing the exposed sides of the quartz slides against the exposed sides of the PDMS, and leaving the combined cell on a hot plate at 90°C for 30 minutes [18, 19].

The fluid flow cell was connected through the precut access holes to Tygon® microbore tubing (0.020 inches inner diameter and 0.060 inches outer diameter), with needle tips cut from 0.5-inch gauge needles inserted into the ends of the tubing to provide a stable connection. These tubes were connected to a PU-980 Intelligent HPLC pump (Jasco, UK) to recirculate the sample solution through it.

We also designed and built a 3D printed photobleaching unit consisting of industrial diode lasers that could be used to reduce the background fluorescence in Raman spectroscopy without wasting the life span of the instrument laser. Details of the design of the unit and dimensions can be found in the “Supplementary Materials” section (Figures S2–S6).

2.3. Experimental Procedures

2.3.1. Fluorescence Recovery Experiments. The experiments were conducted using the fluorimeter by exciting only the tryptophan residues in BSA using 295 nm excitation wavelength and measuring its emission band at 340 nm [20, 21]. For these experiments, a 1 mg·ml⁻¹ solution of BSA in a 3 mm pathlength quartz cuvette (Starna, UK) was photobleached for 10 min with a spectrum measured after each minute. 10 individual measurements were collected using a 3 nm bandwidth for both the excitation and the emission slits, and the photobleaching was conducted with a 10 nm bandwidth for the excitation slit. The sample was then homogenised using a vortex stirrer, and the experiment was repeated.

2.3.2. Photobleaching Experiments Using PDMS Cast. For this experiment, different aliquots of the 40 mg·ml⁻¹ BSA stock solution were measured with the ChiralRAMAN-2X™ spectrometer using a 532 nm excitation wavelength and control unit nominal powers in the range 250–900 mW (~55% at sample position, as measured with a laser power meter by Coherent branded as “Laser Check”). The spectra were exported every 5 min, and the signal at 1838 cm⁻¹ was plotted over time. Two types of experiments were performed:

- (i) No stirring or cooling, with continuous exposure to the laser for ~11 h using 500, 700, and 900 mW control laser powers. 0.080 ml aliquots of the stock solution were measured in a 4 mm pathlength quartz cuvette (Starna, UK).
- (ii) Exposure to the laser while being recirculated through a microfluidic channel for ~11 h using 250 and 500 mW laser powers. Aliquots of ~0.5 ml were required to fully fill the circuit with the pump.

2.3.3. Photobleaching Experiments Using Photobleaching Unit. Aliquots of a 25 mg·ml⁻¹ BSA solution (diluted from the 40 mg·ml⁻¹ stock one to prevent saturation of the detector) were measured using a Thermo Fisher Raman spectrometer, with 633 nm laser, 1s exposure, and 10 accumulations. Then, the samples were photobleached for 30 and 60 min using the external 532 nm and 635 nm lasers and the 633 nm instrument laser in 3 separate experiments, and their spectra were collected using the same parameters as before.

3. Results

The first set of experiments was to investigate the origin of apparent “reversibility” in photobleaching experiments.

In the second set of experiments, we investigated how a recirculating system could be used to remove the recovery artefacts. Finally, we assessed how well our simple external photobleaching unit worked in practice.

3.1. Fluorescence Recovery Experiments. Figure 2 shows how tryptophan fluorescence, measured at 340 nm, decays exponentially with time when exposed to 295 nm light and how significantly (but not completely) the fluorescence signal recovers after mixing with a vortex mixer. This is a consequence of the laser only illuminating a small portion of the bulk of the solution during the experiments and the impurities in the surrounding areas returning to the illuminated area on mixing. Measurements were performed with a small slit aperture to minimise any photobleaching during data acquisition, and the photobleaching was performed with the maximum aperture allowed by the instrument to expose as much area of the cuvette as possible to the radiation.

3.2. Photobleaching Experiments Using PDMS Cast. In order to characterise further the apparent fluorescence recovery after photobleaching in a Raman experiment, a concentrated BSA sample was placed in the BioTools ChiralRAMAN-2X™ instrument which has a more intense laser than most Raman instruments (as it is designed for Raman optical activity). Samples were measured over time using different laser power with and without recirculation. Figure 3 shows how intensity at 1838 cm⁻¹, which was attributed to fluorescence signal only, Figure S7 (Supporting Information), changes over time when exposed to powers between 500 and 900 mW (nominal values).

If the photobleaching process was due only to photo-degradation, the curves in Figure 3(a) could be linearised by applying a logarithm to the data [10]. However, as it can be seen in Figure 3(b), the plot curves become linear to different degrees when expressed on a logarithmic scale with the 500 mW being the most linear followed by 700 mW and 900 mW. We concluded that this trend is due to the fact that higher powers result in more heat and therefore higher thermal degradation.

The fluorescence decay trends for stationary samples in a quartz cuvette shown in Figure 4 initially correspond well to the trends shown in Figure 3(a). However, irregularities were observed in wider time windows. Also, those irregularities occurred earlier for higher powers. To test the hypothesis that this irregular behaviour results from illuminating only small portion of the solution, which locally heats the sample and gives rise to convective currents, we repeated the experiments by recirculating the sample through a homemade PDMS microfluidic device (Figure 1) connected to a HPLC pump, resulting in uniform loss of fluorescence (Figure 4).

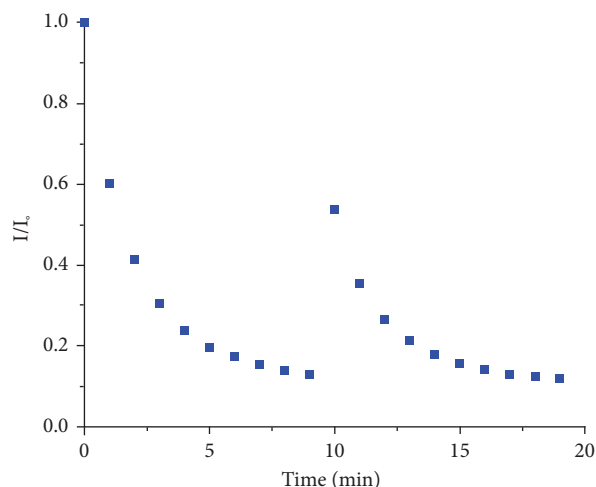


FIGURE 2: Fluorescence recovery after photobleaching of a $1 \text{ mg}\cdot\text{m}^{-1}$ solution of BSA in water. The values of the fluorescence intensity were expressed relative to the initial value.

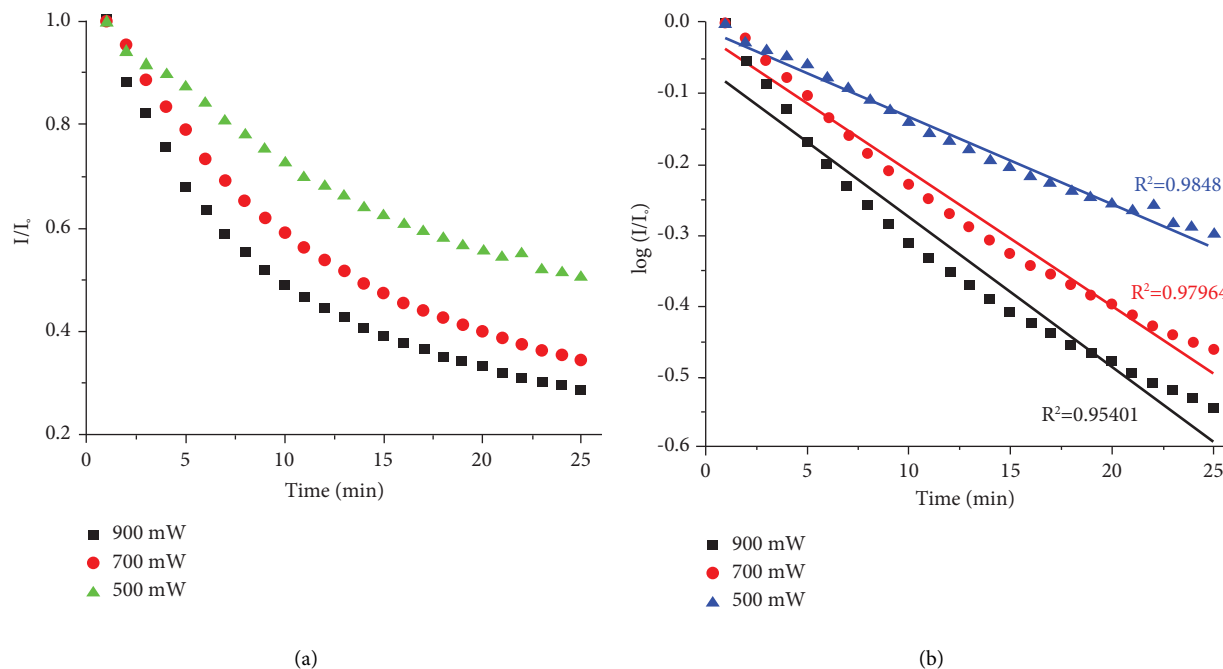


FIGURE 3: (a) Relative Raman intensity at 1838 cm^{-1} (attributed only to fluorescence) of a $40 \text{ mg}\cdot\text{ml}^{-1}$ BSA solution with different nominal laser powers as a function of time with 532 nm excitation in the ChiralRAMAN-2X™ without recirculation. (b) I/I_0 of 900, 700, and 500 mW photobleaching curves in log scale with trendlines overlaid.

3.3. Photobleaching Experiments Using Photobleaching Unit.

While photobleaching in both spectrometers was clearly successful, it is not convenient as it takes 12 hours for a single sample, making the instrument unusable for data collection and reducing the operating lifetime of the instrument. We therefore designed and built an external photobleaching unit in-house. The unit consists of two industrial diode lasers (532 nm , 160 mW output power, and 635 nm , 190 mW output power), purchased from O-like (China). The lasers are enclosed within a 3D printed black case (Figure 5) and a safety interlock to prevent the laser from being exposed during operation. The cross section of the green laser beam

was found to be circular, with approximately 3 mm diameter at sample position. The red laser beam was found to be elongated in the horizontal axis, with the beam cross section at sample position being ellipsoidal ($3 \text{ mm} \times 6 \text{ mm}$). The unit is powered with 12 V DC current. The dimensions of the unit are $14 \times 12 \times 4 \text{ cm}^3$, and the weight is 396 g . The total cost of building the device was approximately $\text{£}200$ (USD\$275).

The device was used to photobleach BSA samples over 30 and 60 min periods using 635 nm and 532 nm external lasers. The results were compared to photobleaching using the 633 nm Thermo Fisher instrument laser. Samples were not mixed in these experiments.

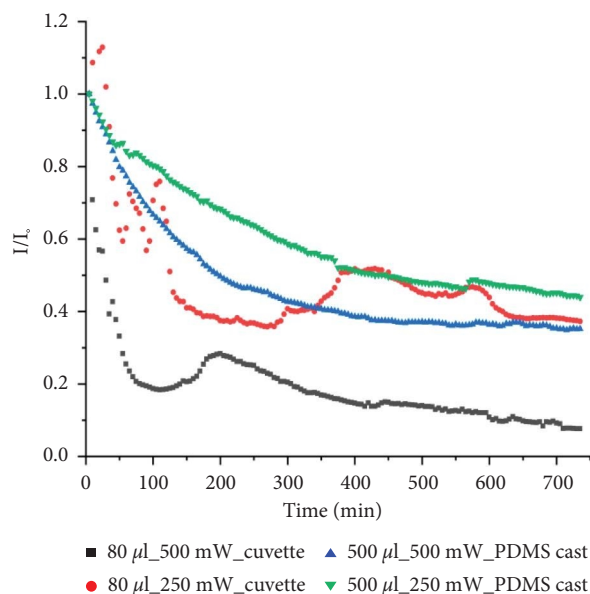


FIGURE 4: Photobleaching of 80 μl of BSA sample in a static cuvette at 500 mW (black square) and 250 mW (red circle) laser power and 500 μl of BSA sample recirculated in a microfluidic device at 500 mW (blue triangle) and 250 mW (green triangle) laser power. The intensities were expressed relative to the initial value as in Figure 3.

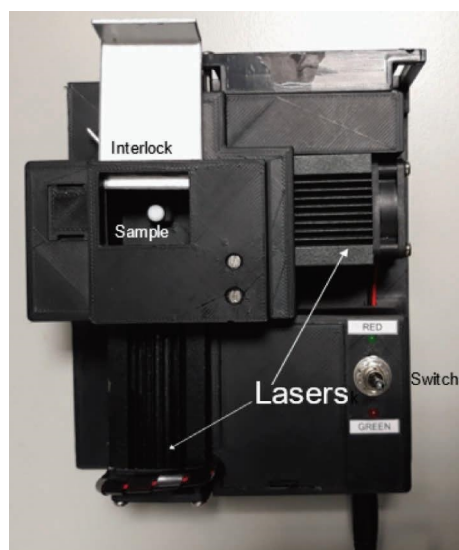


FIGURE 5: Homemade photobleaching unit equipped with a green and a red diode laser.

Figure 6 shows the initial Raman spectrum and how it changes over time when exposed to light. Over the first 30 min, the average background fluorescence was cut down by $\sim 20\%$ and $\sim 15\%$, and over the following 30 min, by an additional $\sim 10\%$ and $\sim 5\%$ when photobleached with the 532 and 635 nm external lasers, respectively. In the case of the instrument laser, the fluorescence dropped by $\sim 25\%$ after 30 min and by an additional $\sim 5\%$ over the following 30 min.

The local fluorescence decrease is highest for the built-in instrument laser, despite its lowest power, followed by the 532 nm and the 635 nm lasers. This observation can be explained by the fact that the cross section of the instrument laser is much smaller (~ 0.5 mm diameter at focal point), and thus the light intensity at the measurement spot is higher. Additionally, this sample was not moved between photobleaching and the measurement, unlike the

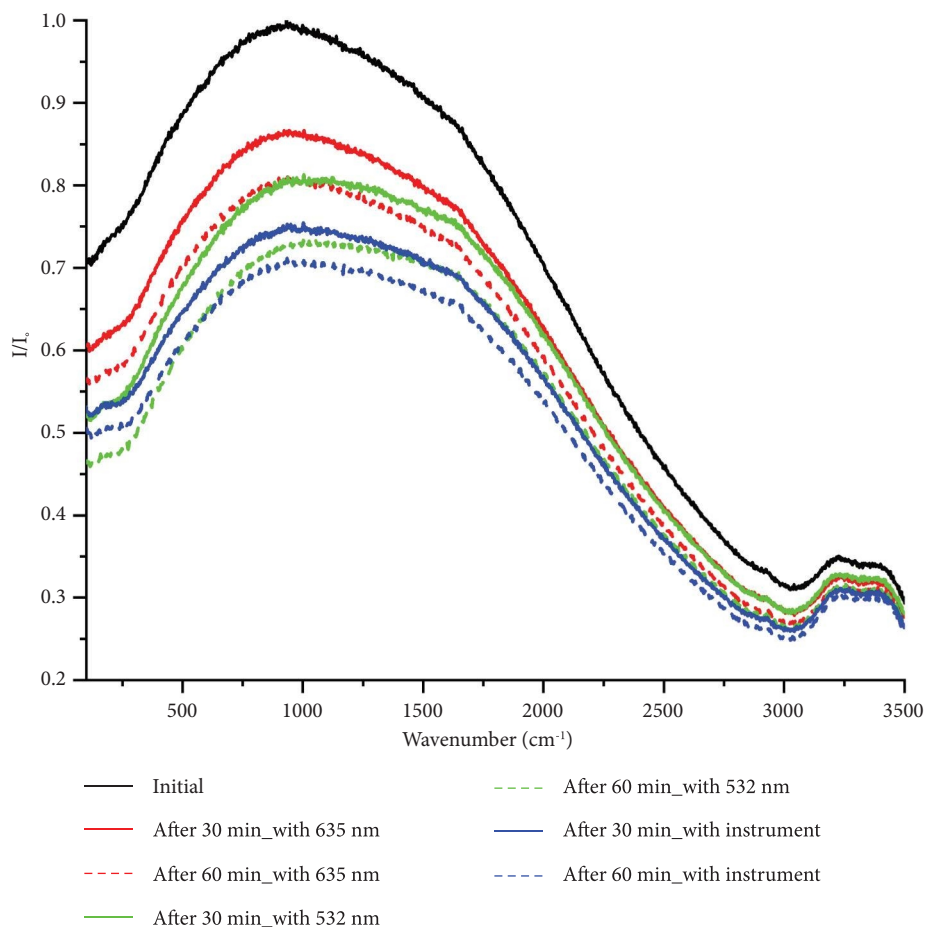


FIGURE 6: Initial spectrum of BSA and after 30 and 60 min of exposure to external 635 nm laser and 532 nm laser and to 633 nm Thermo Fisher Raman spectrometer laser. All the spectra were measured with 1 s exposure and accumulated 10 times. The spectra were expressed relative to the initial values.

samples photobleached externally, which had to be transferred into the instrument and would have undergone some degree of mixing. 60 minutes of external 635 nm laser is approximately equivalent to 30 minutes in the instrument.

Extended photobleaching (3 days) with the external 532 nm laser reduces the fluorescence by a factor of 4 and shifts its wavelength to longer wavelength (Figure 7). In this

case, the curves are indicative of the presence of more than one fluorophore, one of which is removed somewhat more effectively than the other.

We chose 72 h of photobleaching with 532 nm as it enabled a good Raman spectrum to be collected with either Raman spectrometer using the total spectrometer time used of approximately 30 minutes, illustrating the benefit of using external photobleaching process.

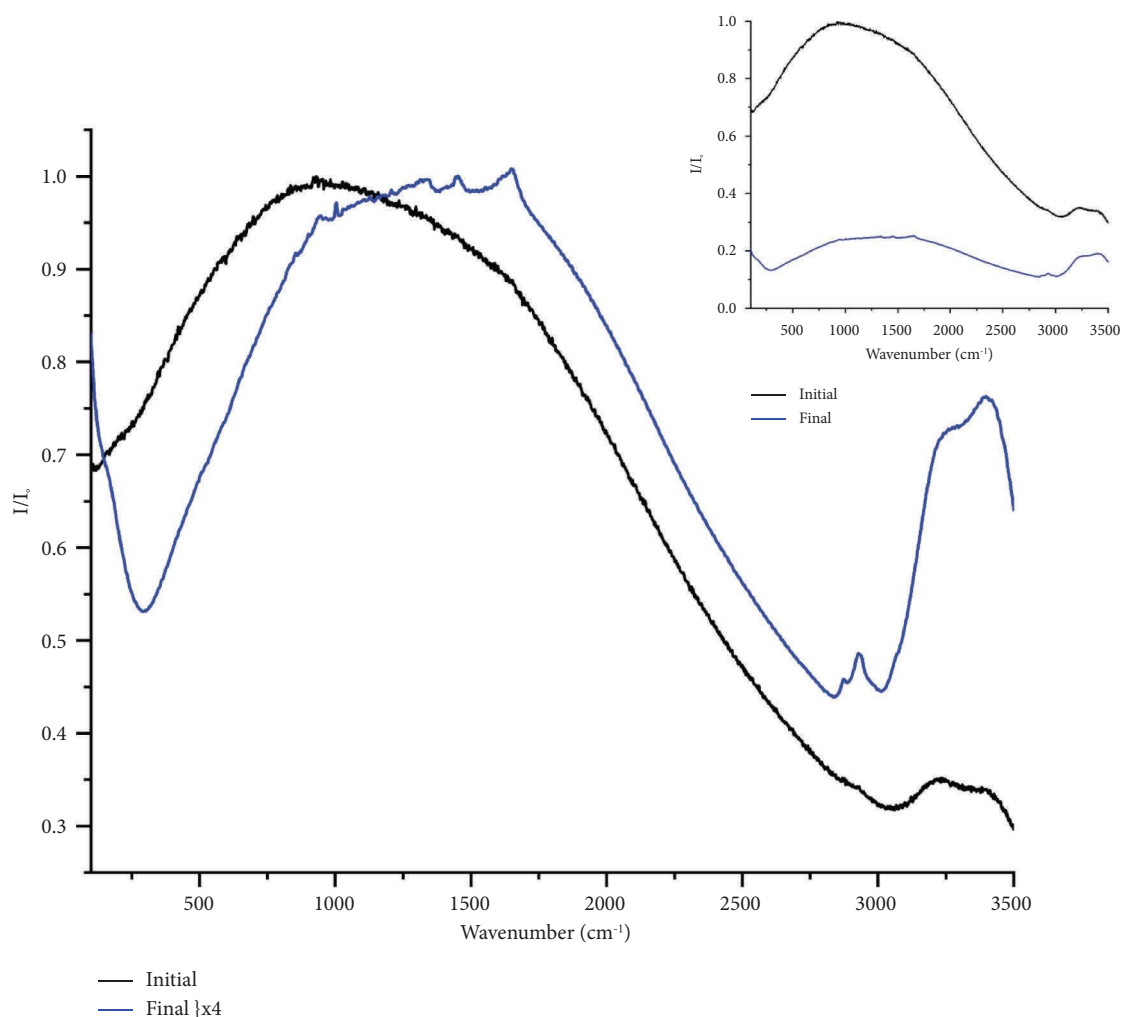


FIGURE 7: Initial BSA spectrum measured with 1 s exposure and 10 accumulations and final BSA spectrum ($\times 4$) after 72 h of photobleaching with the 532 nm external laser measured with 10 s exposure and 200 accumulations. Inset shows the two spectra without scaling.

4. Conclusion

We have demonstrated that, in line with previous reports, the photobleaching process proceeds with exponential decay of the fluorescence intensity. The rate of decay depends on the wavelength, the laser power used, and the identity of the fluorophore. We have also demonstrated that the apparent “reversibility” is the product of restricting the light exposure to small areas of the sample where, by diffusion or mechanical mixing, other fluorophores can migrate, resulting in recovery of fluorescence as in “fluorescence recovery after photobleaching” (FRAP) imaging experiments [22].

We also observed an irregular recovery of fluorescence over extended periods of photobleaching that can be explained by the occurrence of convective flows from local heating of the sample in a cuvette. Those irregularities can be prevented by recirculating the sample with a simple microfluidic flow device. Alternatively, mechanically stirring would have the same effect.

Finally, we have demonstrated that samples can be photobleached externally by means of affordable industrial LED lasers that can be safely used when built into a 3D

printed case with a safety interlock. The external photobleaching unit saves wasting significant instrument time and thus prolongs the instrument’s usable life. The LED laser used in the construction of the external unit had nominal power between 160–190 mW. Higher power LED lasers are available and have potential to further shorten the experiment time.

Data Availability

The data that support the findings of this study are available on request from the corresponding author. The data are not publicly available due to privacy or ethical restrictions.

Conflicts of Interest

The authors declare that they have no conflicts of interest.

Acknowledgments

This study was supported by funding from the Engineering and Physical Sciences Research Council via the Molecular Analytical Sciences Centre for Doctoral Training for MP (no. EP/L015307/1).

Supplementary Materials

Figure S1: dimensions of silicon mask. Figure S2: photobleaching unit through top. Figure S3: photobleaching unit assembly. Figure S4: photobleaching exploded view. Figure S5: photobleaching unit see through. Figure S6: laser's distance to sample in photobleaching unit. Figure S7: Raman spectrum of a $\sim 70 \text{ mg}\cdot\text{ml}^{-1}$ BSA solution collected with the BioTools instrument. The sample was photobleached with 800 W (X 0.55 at sample position) for $\sim 3 \text{ h}$ prior to the measurement and accumulated over $\sim 8.6 \text{ h}$. (Supplementary Materials)

References

- [1] D. Wei, S. Chen, and Q. Liu, *Review of Fluorescence Suppression Techniques in Raman Spectroscopy Review of Fluorescence Suppression Techniques in Raman Spectroscopy*, p. 4928, 2015.
- [2] S. C. Tan and B. C. Yiap, "DNA, RNA, and protein extraction: the past and the present," *Journal of Biomedicine and Biotechnology*, vol. 2009, pp. 1–10, 2009.
- [3] J. Briggs and P. R. Panfili, "Quantitation of DNA and protein impurities in biopharmaceuticals," *Analytical Chemistry*, vol. 63, no. 9, pp. 850–859, 1991.
- [4] D. Wei, S. Chen, and Q. Liu, "Review of fluorescence suppression techniques in Raman spectroscopy," *Applied Spectroscopy Reviews*, vol. 50, no. 5, pp. 387–406, 2015.
- [5] A. M. Macdonald and P. Wyeth, "On the use of photobleaching to reduce fluorescence background in Raman spectroscopy to improve the reliability of pigment identification on painted textiles," *Journal of Raman Spectroscopy*, vol. 37, no. 8, pp. 830–835, 2006.
- [6] P. Vandenaabeele, *Practical Raman Spectroscopy*, 2013.
- [7] J. Kostamovaara, J. Tenhunen, M. Kogler, I. Nissinen, J. Nissinen, and P. Keranen, "Fluorescence suppression in Raman spectroscopy using a time-gated CMOS SPAD," *Optics Express*, vol. 21, no. 25, Article ID 31632, 2013.
- [8] P. McPhie and J. R. Lakowicz, *Principles of Fluorescence Spectroscopy*, 2000.
- [9] P. Praktikum and F. Quenching, "Fluorescence quenching studies," *Physics Prakt.*, pp. 1–14, 2016.
- [10] F. Bonnier, S. Ali, P. Knief et al., "Analysis of human skin tissue by Raman microspectroscopy: dealing with the background," *Vibrational Spectroscopy*, vol. 61, pp. 124–132, 2012.
- [11] F. Bonnier, A. Mehmood, P. Knief et al., "In vitro analysis of immersed human tissues by Raman microspectroscopy," *Journal of Raman Spectroscopy*, vol. 42, no. 5, pp. 888–896, 2011.
- [12] M. Tatarikovi, A. Synytsya, and L. Ští, *The Minimizing of Fluorescence Background in Raman Optical Activity and Raman Spectra of Human Blood Plasma*, pp. 1335–1342, 2015.
- [13] A. Diaspro, G. Chirico, C. Usai, and P. Ramoino, "Photobleaching," 2010.
- [14] J. Widengren and R. Rigler, "Mechanisms of photobleaching investigated by fluorescence correlation spectroscopy," vol. 4, pp. 149–157, 1996.
- [15] J. B. Pawley, *Handbook of Biological Confocal Microscopy*, 2006.
- [16] J. Zi and A. Michalska, "Vibrational Spectroscopy Photobleaching as a useful technique in reducing of fluorescence in Raman spectra of blue automobile paint samples," vol. 74, pp. 6–12, 2014.
- [17] C. Mcdona, H. Un, H. Un, Un, and H. P ol y, "(dimethylsiloxane) as a material for fabricating," 2002.
- [18] S. H. Tan, N. T. Nguyen, Y. C. Chua, and T. G. Kang, "Oxygen plasma treatment for reducing hydrophobicity of a sealed polydimethylsiloxane microchannel," *Biomicrofluidics*, vol. 4, no. 3, pp. 032204–032208, 2010.
- [19] B. Kim, E. T. K. K Peterson, and I. Papautsky, "Long-term stability of plasma oxidized PDMS surfaces," *Annual International Conference IEEE Engineering Medicine Biology - Proceedings*, vol. 2004, pp. 5013–5016, 2004.
- [20] Y. Hui, X. Xue, Z. Xuesong, and W. U. Yan, "Intrinsic fluorescence spectra of tryptophan," *Tyrosine and Phenylalanine*, pp. 224–233, 2015.
- [21] A. B. T. Ghisaidoobe and S. J. Chung, *Intrinsic Tryptophan Fluorescence in the Detection and Analysis of Proteins: A Focus on Förster Resonance Energy Transfer Techniques*, pp. 22518–22538, 2014.
- [22] M. Hof, R. Hutterer, and V. Fidler, *03 Fluorescence Spectroscopy in Biology*, 2004.